Radiocarbon, Vol 58, Nr 1, 2016, p 213–225 DOI:10.1017/RDC.2016.5

INVALIDATION OF THE INTRACAVITY OPTOGALVANIC METHOD FOR RADIOCARBON DETECTION

Cantwell G Carson[1,2]* • Martin Stute[3] • Yinghuang Ji[1] • Roseline Polle[4,5] • Arthur Reboul[4,6] • Klaus S Lackner[1,7]

[1]Earth and Environmental Engineering Department, Columbia University, New York, New York, USA.
[2]National Energy Technology Laboratory, U.S. Dept. of Energy, Pittsburgh, Pennsylvania, USA.
[3]Department of Environmental Science, Barnard College, New York, New York, USA.
[4]École Polytechnique, Palaiseau, Île-de-France, France.
[5]Imperial College London, London, UK.
[6]Neoen, Paris, Île-de-France, France.
[7]The Center for Negative Carbon Emissions, Arizona State University, Tempe, Arizona, USA.

ABSTRACT. The intracavity optogalvanic spectroscopy (ICOGS) method has been reported to quantify radiocarbon at subambient levels (<1 part per trillion). ICOGS uses a gas sample that is ionized in a low-pressure glow discharge located inside a $^{14}CO_2$ laser cavity to detect changes in the discharge current under periodic modulation of the laser power to determine the $^{14}CO_2$ concentration of the sample. When claims of detection thresholds below ambient levels were not verified by other researchers, we constructed a theoretical analysis to resolve differences between these conflicting reports and built and tested an ICOGS system to establish a lower limit of detection. Using a linear absorbance model of the background contribution of $^{12}CO_2$ and data from the HITRAN database, we estimate that the limit of detection ($3\sigma_x$) is close to 1.5×10^4 Modern. By measuring a 1.5×10^4 Modern enriched CO_2 sample in a cavity modulation ICOGS system without a clear signal, we conclude that for this system the limit of detection for ICOGS must be above 1.5×10^4. The implications for previous ICOGS reports are discussed.

KEYWORDS: Intracavity optogalvanic spectroscopy (ICOGS), radiocarbon, laser spectroscopy, monitoring verification and accounting.

INTRODUCTION

Background

Radiocarbon is one of the most important isotopes in modern science and its measurement at ambient levels is critical to fields from archaeology to climatology, but with requirements for detection necessary well below the 1.23-part-per-trillion ambient concentration (1 Modern), the ratio of ^{14}C to ^{12}C is not easy to quantify (Hellborg and Skog 2008; Litherland et al. 2011). Measurement often involves expensive facilities (as in accelerator mass spectrometry) or long count times (as in beta decay counting). Accordingly, there have been several efforts to develop alternative, potentially superior, ways to quantify ^{14}C concentrations at sub-part-per-trillion levels (Povinec et al. 2009). An advancement in this field would have the potential to perform continuous monitoring of atmospheric ^{14}C levels, so as to distinguish biogenic and anthropogenic CO_2.

One such method, intracavity optogalvanic spectroscopy (ICOGS), has been reported to have accomplished this with small sample sizes, real-time detection, and percent-level Modern sensitivity (Murnick and Okil 2005; Murnick et al. 2007, 2008, 2010; Ilkmen and Murnick 2010). In this method, a measurement chamber containing the sample gas is placed at low vacuum inside the cavity of a $^{14}CO_2$ laser. Electrodes on the outside of the chamber then ionize the gas into a low-pressure glow discharge. By placing a chopping wheel between the laser high reflector and the sample cell, the laser periodically modifies the glow discharge. This modification is detected by measuring the impedance of the glow discharge. ICOGS was claimed to have achieved its high sensitivity from the stimulated emission of photons from the 10^4 ^{14}C atoms present in the intracavity beam. The specificity was attributed to the very small intrinsic linewidth of a CO_2 laser. The $^{14}CO_2$ laser then generated a signal on the order of 1 V (after amplification) from a sample of modern CO_2.

*Corresponding author. Email: carsonc@netl.doe.gov.

Following this, other reports have sought unsuccessfully to reproduce these initial and very promising results (Eilers et al. 2013; Persson et al. 2013; Paul and Meijer 2015; Persson and Salehpour 2015). Our own efforts to duplicate these results were also unsuccessful. This pointed to the need to revisit the theoretical foundation of the measurement, and we developed a model to reconcile these conflicting sets of reports.

Theory

For a given glow discharge cell of length L, probed by a laser of cross-sectional area A, at temperature T, the optogalvanic response of a molecule in the discharge is dependent on the concentration, absorbance cross-section, and particular proportionality constant for the specific laser transition being probed. Accordingly, the response of the i^{th} species in a discharge to a laser transition, j, with a given laser profile, $I(v)$, can be represented by a single scalar value, $S_{i,j}$, that is equal to the product of the optogalvanic proportionality constant, $K_{i,j}$, the number of moles present in the active volume (LAp_i/RT), and the integral of the product of laser intensity, $I(v)$, with the absorbance cross-section, $\sigma_i(v)$, evaluated as a function of frequency (v):

$$S_{i,j} = K_{i,j} \frac{LAp_i}{RT} \int I(v)\sigma_i(v)dv$$

Of interest are the optogalvanic responses of $^{12}CO_2$ and $^{14}CO_2$, which we can denote as S_{12C} and S_{14C} respectively. The optogalvanic response as function of laser frequency has been shown to have the same shape as the absorbance profile, but the proportionality constant, $k_{i,j}$, between the optical absorbance profile and the optogalvanic cross-section is unique for each laser transition (Bachor et al. 1982). The $k_{i,j}$ coefficients are not known for $^{14}CO_2$, nor are they known for the many energetically high-lying lines in $^{12}CO_2$ with transitions that might overlay those of the more conventional $^{14}CO_2$ lasing lines. However, for the purposes of developing a first-order model we can assign the value of 1 to all $k_{i,j}$ and examine what would be the relative magnitudes of optogalvanic responses from different species to the same laser stimulation. Experiments can then be carried out to qualitatively determine the relative values of $k_{i,j}$, which have previously been shown to span a factor of about 10 (Bachor et al. 1982).

The line profile for the laser intensity, $I(v)$, can be modeled to first order as a Lorentzian. We can take 300 kHz as the full-width half-maximum of the laser intensity, centered on the $^{14}CO_2$ P(20)e line (25475818.21 MHz, 00011-10001)*, as this corresponds to the coherence length stated by the manufacturer (Freed et al. 1980; Bradley et al. 1986). The intensity and linewidth of the $^{14}CO_2$ P(20)e line has not been reported and its exact measurement remains outside the scope of this paper. However, we can assume it to be similar to the corresponding $^{12}CO_2$ P(20)e line (28306224.9 MHz, 00011-10001), so we will use those values (2.10×10^{-23} cm mol^{-1} wavenumbers per column density and 6 MHz linewidth) as a proxy for the $^{14}CO_2$ P(20)e line (Rothman et al. 2013). $^{12}CO_2$ also happens to have a nearby P(19)e line (25475767.15 MHz, 20001-11102). The efficiency for the P(19)e line for $^{12}CO_2$ at 1.33 mbar and 296 K is 7.89×10^{-26} cm mol^{-1} with a linewidth of 6 MHz (Rothman et al. 2013). Although much weaker, this line is only 52 MHz away from the $^{14}CO_2$ line, or about 8.6 linewidths. Once the positions, linewidths, and intensities of the absorbance lines are known, the frequency-dependent absorbance coefficients, $\sigma_i(v)$, for these two responses can be modeled with the absorbance using parameters from the HITRAN database, using a full Voigt absorbance profile (Rothman et al. 2013). When the laser intensity profile and absorbance coefficients are known, the integrals

*HITRAN notation is used for line transitions.

https://doi.org/10.1017/RDC.2016.5 Published online by Cambridge University Press

thereof can be evaluated to produce an estimate of the relative contribution of the each process to the overall optogalvanic response.

Using this method, we can estimate the unitless pure component signal ratio of S_{14C} to S_{12C} as 9.8×10^3. This number suggests that any detection on the P(20)e line of $^{14}CO_2$ at 1 Modern (1.23 parts-per-trillion) would require a signal to noise level of 2.5×10^8 (assuming a limit of detection definition of $3\sigma_x$). This high level of precision and concurrent dynamic range are uncommon for real-world instrumentation, raising the possibility that the measurements produced at the $^{14}CO_2$ P(20)e were badly confounded by fluctuations in the $^{12}CO_2$ P(19)e optogalvanic response. A variation in the $^{12}CO_2$ P(19)e line as small as 1 part in 10^8 would confound the signal expected from the $^{14}CO_2$ P(20)e line. However, the presence of a strong, $^{12}CO_2$-dependent line can provide an internal reference for evaluating the optogalvanic response of any of the nearby $^{14}CO_2$ lines. For example, this same analysis can be carried out for the nearby $^{14}CO_2$ P(24)e line (25371973.5 MHz, 00011-10001) (Freed et al. 1980; Bradley et al. 1986). This line has an overlap with the $^{12}CO_2$ Q(13)e line (25371968.2, 32202-31103), but the efficiency of this line (1.33 mbar, 296 K) is 2.0×10^{-30} cm mol^{-1} with a linewidth of 51 MHz (there are no $^{13}CO_2$ lines in this region to examine). This produces an equivalent optogalvanic ^{12}C to ^{14}C ratio of 8.5×10^6, resulting in a signal-to-noise ratio of 2.9×10^5 at the $^{14}CO_2$ P(24)e line necessary to detect the presence of $^{14}CO_2$ at ambient levels above the background $^{12}CO_2$ at this line. As a result, even though the P(24)e line is weaker, the contribution from $^{14}CO_2$ to the optogalvanic effect can be much more pronounce because the interference from $^{12}CO_2$ is much more attenuated. Figure 1 shows a comparison between the expected contributions from $^{12}CO_2$ and $^{14}CO_2$ at P(20)e and P(24)e as a function of wavelength offset from the laser frequency.

It is important to note that this analysis relies neither on the intensity of laser stimulation nor the presence of any intracavity enhancement. Although a greater laser power or hypothesized path length enhancement will no doubt increase the optogalvanic voltage measured, it will do so for all

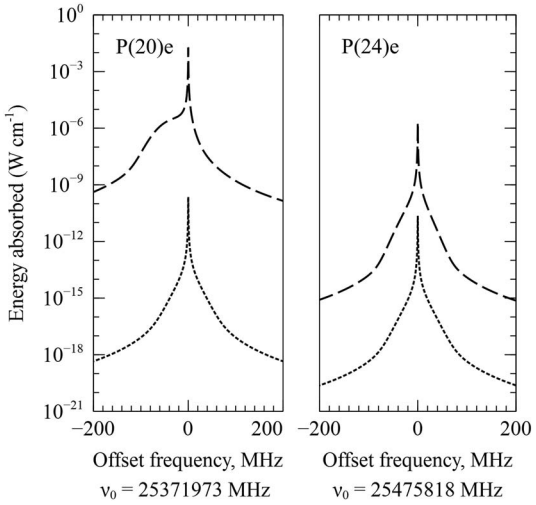

Figure 1 The theoretical absorbance profiles for pure $^{12}CO_2$ (dashed lines) and for a 1 Modern concentration of $^{14}CO_2$ (dotted lines) for a $^{14}CO_2$ laser operating at the P(20)e line (left) and the P(24)e line (right). The contribution of P(19)e is clearly visible in the asymmetry of the $^{12}CO_2$ response to a $^{14}CO_2$ P(20)e laser line.

https://doi.org/10.1017/RDC.2016.5 Published online by Cambridge University Press

components present in the system and the resulting ratios will remain roughly constant. Changes in temperature or pressure would affect the line broadening of the absorption profile and changes in the linewidth of the laser would also affect the expected signal ratios. Variations of the optogalvanic signal in excess of $1{:}10^8$ are likely due to fluctuations in the ^{12}C response rather than due to a ^{14}C signal.

To test this analysis, a survey of $^{14}CO_2$ laser lines around P(20)e at a highly enriched ^{14}C level was conducted to determine whether the ICOGS method might supply the requisite sensitivity on a different line. For example, according to the above analysis, the 0.5 V/V signal reported by Murnick et al. (2010) on P(20)e is unlikely to reflect a $^{14}CO_2$ signal as it should have been contributing only 2 nV/V if $^{14}CO_2$ is present at the 1-part-per-trillion level. That such a large signal of 0.5 V/V was observed where only a tiny fraction could have actually correlated to the desired $^{14}CO_2$ is highly indicative that the signal measured did not actually originate from $^{14}CO_2$, but rather some other part of the experiment, such as temperature or pressure fluctuation. Looking at the data presented by Murnick, the estimated pure component ratio of S_{14C} to S_{12C} would be 5.7×10^{11}, over 50 million times greater than what would be expected based on this cursory analysis.

One way to resolve this discrepancy would be to generate a sample of CO_2 enriched with $^{14}CO_2$ to a level of 5×10^7 Modern. Measuring such a sample near any facility that also works with ^{14}C at subambient levels would entail a serious threat to the integrity of surrounding research projects in the event of an accidental release. Accordingly, a level of 1.5×10^4 Modern was agreed upon as being high enough to potentially determine an upper limit of detection for ^{14}C yet low enough to ensure the integrity of surrounding laboratories. If a signal is measured with a high precision, then the $K_{14CO2,P(24)e}$ is much larger than $K_{12CO2,P(19)e}$. Conversely, the absence of a signal would indicate the reverse.

EXPERIMENTAL METHODS

Laser Optics and Arrangement

The laser beam path and gas line plumbing for the experiment are schematically shown in Figure 2. The laser was the Merit-SZ from Access Laser Inc. (Everett, WA), modified with an extended cavity and filled with a custom gas mixture containing $^{14}CO_2$ (60 mCi/mmol) from ViTrax Inc. (Placentia, CA). An output coupler with 1% transmittance at 11.8 μm was used to increase the finesse of the cavity. A cross-cell placed inside the extended cavity was used as the sample chamber, consisting of a 2.54×2.54 cm (D × L) glass tube along the laser axis and a 1×5 cm (D × L) glass tube horizontally perpendicular to the first. The ZnSe windows used in the cross-cell were AR-coated to maximize transparency at 11.8 um (II-IV Inc., 398438). The laser cavity length was controlled by a piezo-electric crystal mounted to the high reflector (gold-coated front face mirror, 1-m radius). The driver for the piezo-electric crystal was a Thorlabs Inc. (Newton, NJ) MDT693B open loop piezo controller with a maximum voltage of 150 V. To set the piezo controller voltage, a National Instruments (Austin, TX) 9263 Analog Output Module was used, as was the piezo controller's serial RS-232 interface. The average laser power was measured with an Ophir Optronics (Jerusalem, Israel) 3A power meter attached to a Juno USB interface. To measure the high-speed modulation in laser power (>1 Hz), a portion of the laser beam output was reflected into a QS-V-TEST Evaluation test box with a QS9-VL fast response discreet pyrometer from Gentec-EO (Quebec City, Canada). The output of the QS-V-TEST was sampled by a National Instruments 9215 analog input module with a sampling rate of 50 kHz. The laser wavelength was measured with a spectrum analyzer from Macken Instruments Inc. (Santa Rosa, CA). The position of the laser line in the spectrum analyzer was determined by images taken with a FLIR i3 infrared camera (Boston, MA).

https://doi.org/10.1017/RDC.2016.5 Published online by Cambridge University Press

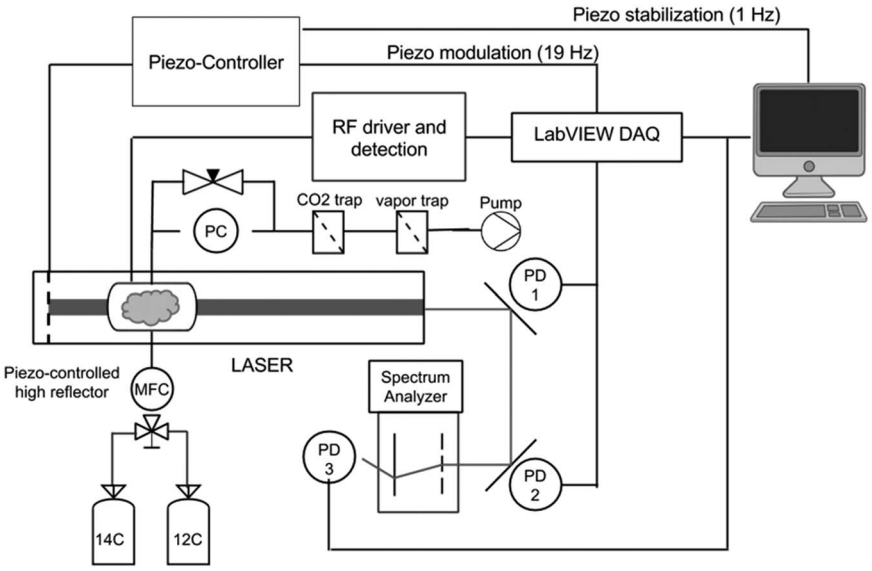

Figure 2 A schematic diagram of the experimental apparatus is shown. The laser output power, modulation amplitude and phase, and wavelength are all monitored with a thermopile, photodiode, and infrared camera at PD 1, 2, and 3, respectively.

Circuitry and Power Considerations

The circuit board used to drive the low-pressure glow discharge at 10 MHz was produced according to previously published designs. The output stage of the radiofrequency (RF) driver consisted of a pair of homodyne demodulating rectifiers, 180° out of phase, with a low-pass RC filter and a 3.3-kHz cutoff. A differential amplifier was designed to demodulate the outgoing RF signal down to audio frequencies. The differential amplifier featured a high-pass first-order RC filter with a cutoff frequency of 1 Hz followed by a fourth-order low-pass Sallen-Key Chebyshev filter with a 1-kHz cutoff frequency and an instrumentation amplifier with a gain of 1000. The schematics, circuit board layouts, and lists of materials for these boards are presented in the Online Supplementary Material. The differential amplifier was also connected to the analog input module and sampled at 50 kHz. The circuit boards were powered by a National Instruments PXI-4110 triple output programmable power supply. Additional current for the PXI-4110 was supplied by a TDK-Lambda Americas (San Diego, CA) SCD601515 15V dual output power supply.

Signal Generation

The optogalvanic signals were generated by modulating the laser cavity length using a sawtooth wave at 19 Hz and 15 V. These signals were generated at the analog output module, amplified by the piezo controller, and then used to modulate the cavity length. To detect the effect of this cavity modulation, a coherent averaging algorithm was used to extract the optogalvanic component of the signal. In this case, the coherent average was produced by averaging 19 consecutive cycles collected over a single second together. The amplitude of optogalvanic signal was calculated from the first non-DC harmonic of the fast Fourier transform (FFT) of the coherent average. This same algorithm was used to calculate the phase and amplitude of the laser power measurement from the fast response pyrometer. To compensate for thermally

https://doi.org/10.1017/RDC.2016.5 Published online by Cambridge University Press

induced changes in cavity length during long, continuous measurements, a control loop was implemented whereby the offset voltage applied to the piezo controller could be adjusted to keep the phase of the fast response pyrometer at a constant value.

The laser was tuned to produce the P(20)e and P(24)e $^{14}CO_2$ peaks, which were verified by observation in the spectrum analyzer through the infrared camera. The laser was then operated in a high-resolution slow scanning mode, where the offset voltage on the cavity modulating signal was increased stepwise through the total range of the piezo controller (100 V) at 0.5-V steps with 1-s durations. Consecutive high-resolution scans were then aligned to compensate for small thermally induced changes in the width of the longitudinal modes between scans. The measured optogalvanic voltages were divided by the laser power and by the pressure to compensate for laser power and pressure variation between runs (both samples were kept in Mylar bags to eliminate the variation of backpressure between samples). The optogalvanic responses were then normalized to a peak signal of 1 to highlight variation between samples outside of the $^{14}CO_2$ P(20)e laser line (<40 V PZT). The data were then averaged with a 6-point low-pass filter to attenuate point-to-point variation. A 1-hr scan was also performed on the P(24)e peak with dead CO_2 to determine the long-term stability of the measurement. Mass flow controllers from MKS (Andover, MA) were used at 1 cm^3 min^{-1}. The cell outlet was connected to a pressure controller (MKS), at 1.33 mbar.

Sample Handling

The reference gas used was UHP CO_2 from Tech Air and the ^{14}C content of the calibration gases used was measured separately at the BioAMS facility at Lawrence Livermore National Labs. To make a highly enriched tracer, we designed and constructed a gas-liquid tracer tag filling station. The content of the stainless steel tracer tag was injected into 750 mL of dead CO_2 in a gas bag and allowed to equilibrate with gentle shaking overnight. The ^{14}C-enriched CO_2 was then passed into a fresh gas bag through a dry ice/ethanol cold trap to remove residual water vapor. Samples of the ^{14}C-enriched CO_2 were taken and diluted to 0.1% in dead CO_2 before being shipped off for measurement.

RESULTS

Figure 3 shows a comparison between the amplifier used in the original results reported by Ilkmen and Murnick (2010) and that used in the present work. When the laser is optically chopped, a large, transient spike appears shortly after the laser turns on and off in the amplifier used in the present work. This spike is absent in the signal from the previously used amplifier, even though the optical chopping was used, due to the low-pass filter present on earlier designs. The fast components were, of course, still present, yet were being confounded with the rest of the lower-frequency response. The offset between the two outputs during the "laser on" stage arises from a difference in the high-pass filter stage of the amplifier, but is not otherwise meaningful.

Figure 4 shows the comparison between sequential measurement of dead and enriched CO_2 samples. These scans were taken 5 min apart. First, the dead sample was measured and then the enriched sample was measured afterwards. The peak at P(20)e appears doubled because the cavity modulation method used to generate the ICOGS signal is partially sensitive to the absolute value of the first derivative of the ICOGS signal. The other peaks are too small to resolve any equivalent doubling. Accordingly, Figure 4 also shows the results of a single exponential peak fit of a Gaussian of the form $S_{fit} = A_0 e^{-(V-V_0)^2/2b^2} + c$ on the P(24)e peak, between 45 and 80 V for both samples. Here, A_0 is the peak height; V_0 and V are the peak piezo

https://doi.org/10.1017/RDC.2016.5 Published online by Cambridge University Press

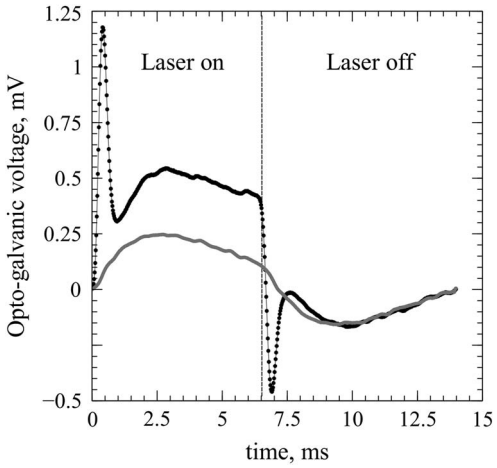

Figure 3 The comparison of the differential amplifier used in the original results (gray) and that used in the present work (black). Note the sharp spike at shortly after the laser switches on and off.

voltage and control piezo voltage, respectively; *b* corresponds to the peak width; and *c* is the minimum measured signal. These fits were then integrated numerically at 1 standard deviation above and below the fitted parameters. These integrals were then used to establish the estimated area under the curve and the uncertainty of that estimate. The difference between the integrated enriched and dead signals divided by the root-mean-squared sum of the uncertainties produced an estimated significance of $2\sigma_x$.

DISCUSSION

Figure 3 highlights the first indication that the original results as to the sensitivity to $^{14}CO_2$ might be questionable. The original amplifier was designed to filter out common mode and high-frequency fluctuations between two RF amplitude inputs from the optogalvanic discharge board (see Figures S3 and S4 in the SOM). On the original circuit boards, the passive first-order low-pass filters on the differential amplifier had a cutoff frequency of 75 Hz. When we were able to replace this with an amplifier that had a cutoff frequency of 1 kHz, we immediately saw a sharp spike when the laser would turn on or turn off. When the glow discharge was subjected to large power fluctuations, as occur inside an optically chopped laser cavity, a fast, broadband relaxation process occurs, previously obscured by the 75-Hz low-pass filter. These artifacts are so pronounced that they call into question whether $^{14}CO_2$ could have ever been detected at all in this fashion. This led to the development of the cavity modulation method, which eliminated most of the artifact arising from the large changes in applied power while chopping the laser.

The cavity modulation allowed for a more sensitive approach to optogalvanic spectroscopy that might be better suited to detecting very small signals. This was the case, as can be seen in Figure 5 from the minimum 37-ppm deviation [relative to the full-scale P(20)e measurement at 1000 s integration time] estimated from the Allan deviation curve. This would have the potential to produce a signal-to-noise ratio as high as 2.7×10^4. Even with this high sensitivity, it would be impossible to see the P(20)e line behind the P(19)e line of the $^{12}CO_2$ at ambient levels, which are about 8 orders of magnitude larger in strength. This level of signal quality may by sufficient at

https://doi.org/10.1017/RDC.2016.5 Published online by Cambridge University Press

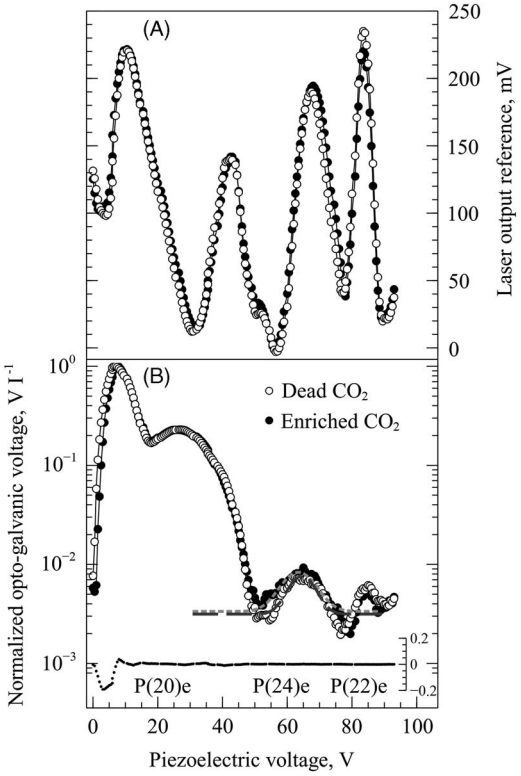

Figure 4 (A) The amplitude of the modulation in the output of the laser, as measured by the fast response pyrometer. (B) The optogalvanic response is shown with a log scale on the *y* axis. Beneath these, the difference between the two samples is shown on a linear *y* axis (inset, right). Gaussian fits of two samples (dashed line and dotted line) at P(24)e are also shown for the dead and enriched samples, respectively.

P(24)e, where the $^{12}CO_2$ signal is relatively much smaller. Due to the P(24)e diminished size, a 37-ppm at 1000-s integration time deviation would produce a signal-to-noise ratio of 85. The collection time during the P(24)e peak was approximately 54 s, reducing the expected signal-to-noise ratio to 19 in the region of interest. At this signal-to-noise level at P(24)e, we should be able to detect 1.5×10^4 Modern ($3\sigma_x$) and quantify 5.0×10^5 Modern ($10\sigma_x$) (Shrivastava and Gupta 2011). Whether this is true in reality will in part depend on the actual values of the $K_{i,j}$ coefficients, which could modify the signal ratios by about an order of magnitude.

Analysis of the data in Figure 4 show that a confidence level of $2\sigma_x$ was obtained for 1.5×10^4 Modern with a Gaussian fit function and some filtering of the data. Given the low confidence interval, it is clear that a limit of detection threshold was not reached and that the real limit of detection in this experiment must be higher than 1.5×10^4 Modern. Even the small difference of 0.13% measured at 55 V has a potential confounder at that same location in the laser output profile as measured with the fast-response pyrometer. The graph in Figure 6 compares this result to those in two previously published reports by Murnick et al. (2008, 2010) and

https://doi.org/10.1017/RDC.2016.5 Published online by Cambridge University Press

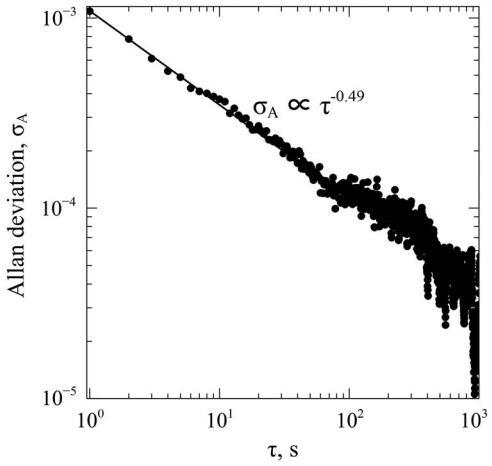

Figure 5 An Allan deviation curve collected at the P(24)e line of $^{14}CO_2$ is shown for the ^{14}C-enriched sample. Over the first 100 s, the deviation decreases as $\tau^{-0.49}$, which is consistent with white noise. At 1000 s, the deviation is 37 ppm of the signal relative to the P(20)e laser line peak

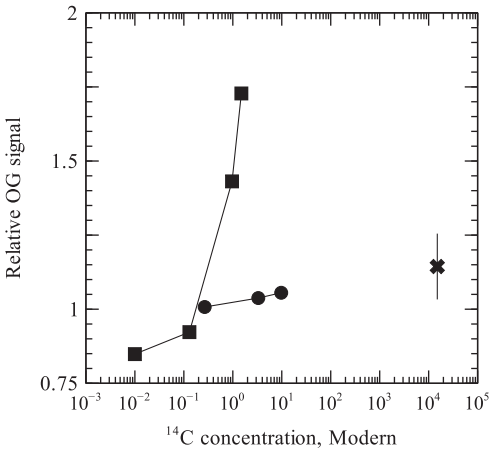

Figure 6 The $^{14}CO_2$ optogalvanic signal relative to that of dead CO_2 is shown as a function of ^{14}C concentration for results from three different publications, Murnick et al. (2010) at P(20)e (■), Eliers et al. (2013) at P(20)e (●), and the present results at P(24)e (✖). The pressures for the three results were 1, 1, and 1.3 mbar, respectively.

Eliers et al. (2013), respectively. Clearly, although our signal generation method and laser line differs from that of Eliers, our results are much more in line with theirs than those of Murnick.

These results illustrate how earlier studies claiming part-per-trillion sensitivity for the ICOGS method could have produced misleading results. Given the more complete picture of the superposition of $^{12}CO_2$ and $^{14}CO_2$ lines, it is understandable why there would appear an

https://doi.org/10.1017/RDC.2016.5 Published online by Cambridge University Press

enormous response at the P(20)e $^{14}CO_2$ laser line. A fluctuation or drift of the optogalvanic response at the P(20)e line, such as might be caused by a slight temperature or pressure change, could be interpreted to constitute a response from changing $^{14}CO_2$ levels even though they reflect changes in the $^{12}CO_2$ response. This is possible because, unlike in spectroscopic methods, the optogalvanic response provides no method to differentiate between the different contributors to the response. The optogalvanic response can be either positive or negative, depending on how the laser affects the population inversion in the sample. As a result, neither positive nor negative small deviations can be ruled out as originating from potential confounders on the basis of first principles.

Future efforts to quantify $^{14}CO_2$ optogalvanic responses will have to account for the relative size of the expected signal to the size of the optogalvanic response of nearby $^{12}CO_2$ spectral lines and its sensitivity to small changes in the state of the system. Furthermore, one needs to consider other contributions to the optogalvanic effect, which include the broadband excitation that occurs with high-power laser simulation and RF feedthrough from an RF chopped laser cavity. A discharge cell will often be tuned in the absence of stimulation to minimize the background, but a signal generation method that relies on a chopped laser will be susceptible to one or both of these background sources. By using cavity modulation to generate the optogalvanic signal, the effect of power modulation is dramatically attenuated and the effect of RF feedthrough is eliminated. Although there is a small change in laser power over the course of a scan with cavity modulation, the laser remains on continuously; thus, the change in laser power over the course of a scan is much smaller than would be the case with laser chopping. In addition, because the laser is operated continuously, there is no portion of an RF chop signal that can be folded into the optogalvanic signal. As can be seen in Figure 4, cavity modulation produced a signal-to-background ratio [P(20)e peak-to-minimum of the measurement] of 500. A measurement with a lower signal-to-background ratio may have an even higher limit of detection.

As in Munick's reports, pure CO_2 was used in this study, whereas other studies have also looked at the effect of dilute CO_2 mixtures with N_2. N_2 is used because it possesses a vibrational mode ($\nu = 1$, $E = 2330.7\,cm^{-1}$) $18\,cm^{-1}$ away from the excited state of CO_2 ($\nu = 00011$, $E = 2349.2\,cm^{-1}$) necessary to populate many of the strongest CO_2 lines with very high efficiency, including the P(20)e line. This is a widely understood principle that is applied in many commercial and scientific CO_2 lasers, including our own. Under perfect conditions, the use of N_2 will have the effect of enhancing the response of $^{14}CO_2$ while diluting the effect of $^{12}CO_2$. The upper level of the overlapping $^{12}CO_2$ P(19)e transition ($\nu = 20001$, $E = 2797.1\,cm^{-1}$) is $466\,cm^{-1}$ away from the N_2 vibrational state and is not populated by N_2 the way that the $^{14}CO_2$ P(20)e transition is. If the N_2 were sufficiently efficient at populating the 00011 state to depopulate the other levels of the $^{12}CO_2$ through collisional energy transfer, it might suppress a background signal. However, the high electron temperature inside the glow discharge would make it difficult to completely depopulate any state. Conversely, the high temperature of the electron gas makes it very unlikely that both the upper and lower level of the $^{14}CO_2$ P(20)e transition are completely unpopulated in the absence of N_2. Setting aside the question of whether or not this enhancement alone would be sufficient to make part-per-trillion concentration detectable, dilution with N_2 reduces the number of ^{14}C atoms in the beam, and any N_2 enhancement depends on the concentration, introducing another possibility for fluctuations in the $^{12}CO_2$ optogalvanic response. While this kind of measurement does not pose an insurmountable obstacle, the preliminary characterization of such a sample for the purpose of removing this potential confounder would be substantial. For that reason, we chose instead to focus simply on pure CO_2.

https://doi.org/10.1017/RDC.2016.5 Published online by Cambridge University Press

These results also confirm that path length enhancements invoked to explain the extraordinary response of $^{14}CO_2$ to intracavity optogalvanic stimulation cannot be said to produce the desired selectivity. Electrons in high-lying levels across all species present will contribute to the optogalvanic response, potentially hiding contributions from sub-part-per-billion components, regardless of the quality of the laser or experimental procedure used. Furthermore, the specificity cannot necessarily be enhanced by a narrower laser linewidth, because narrower linewidth does nothing to attenuate the much larger $^{12}CO_2$ absorbance on a nearby line. A full survey of all available $^{14}CO_2$ laser lines could produce a subset of lines that has little to no overlap with high-lying $^{12}CO_2$ or $^{13}CO_2$ lines and these might be good candidates for analysis. However, the voltages produced by 1 part-per-trillion would still be very small as it only involves a handful of molecules. An ICOGS system sensitive enough to (1) quantify a part-per-billion voltage modulation (2) with high statistical significance (3) fast enough to stay within calibration has never been conclusively demonstrated.

It may still be possible that intracavity optogalvanic stimulation can produce ppb sensitivity, as has also been shown with intracavity laser absorption spectroscopy (ICLAS) (Picqué et al. 2005). Berglund and Persson et al. have demonstrated improved sensitivity with very small plasma sources, albeit without quantification of ^{14}C (Berglund et al. 2013, 2014; Persson et al. 2014a, 2014b). Whether or not a system incorporating an ICOGS measurement of a different isotope can compete with existing technologies remains an open question. Our own measurement still requires confirmation by another laboratory, but these highly elevated levels of ^{14}C are already amenable to measurement with beta-decay counting, of which several commercial instruments are already available. Furthermore, Galli and colleagues have already shown sub-part-per-trillion sensitivity to ^{14}C using saturated absorption cavity ring-down spectroscopy (SCAR) (Galli et al. 2011a, 2011b, 2013; Mazzotti et al. 2012).

CONCLUSIONS

The ICOGS method, introduced as a potential ^{14}C measurement technique at ambient concentrations, in the specific implementation of the experiment described here has a limit of detection above 1.5×10^4 Modern, well beyond what would be necessary for ambient samples. This experimental result is in agreement with our theoretical analysis and suggests that the optogalvanic response of a CO_2 sample exposed to laser light from the P(20)e transition in $^{14}CO_2$ has no unusual enhancement but rather is the consequence of the optogalvanic response of the $^{12}CO_2$ in the sample to the nearby P(19)e transition in $^{12}CO_2$, which is expected to be 8 orders of magnitude larger than the 1-Modern $^{14}CO_2$ optogalvanic response of the gas.

The theoretical analysis further suggests that the current experimental method using cavity modulation and a less prominent transition line (P(24)e) is more sensitive to $^{14}CO_2$ than that of Murnick's work. However, given the high excitation of the optogalvanic plasma, it is very unlikely that the absence of nitrogen would completely depopulate the $^{12}CO_2$ excited states that are responsible for the background spectral lines that interfere with the $^{14}CO_2$ signal or for that matter allow for a greatly higher population of the $^{14}CO_2$ states responsible for the transition.

We attribute the previous reports of detection to the presence of a high-lying $^{12}CO_2$ absorbance line that was not noticed and recognized as a confounder. By forming a linear absorbance model for the ICOGS method, we show that the optogalvanic coefficients would have to be 10^9 times greater for the P(20)e line than for the confounding P(19)e transition in $^{12}CO_2$. Drifts in the laser or optogalvanic system could explain the apparent correlation between signal and $^{14}CO_2$ concentration, which in other experiments could not be reconfirmed. The attempts to

https://doi.org/10.1017/RDC.2016.5 Published online by Cambridge University Press

detect $^{14}CO_2$ at the previously reported laser lines have also failed for the same reason. Furthermore, the instrumentation used by Murnick et al. has been shown to introduce artifacts into the measurement that constitute further confounders. In attempting to avoid these errors, we also report a cavity modulation method that eliminates most (but not all) of the laser power fluctuation believed to be partially responsible for the laser power-based confounder. We show that other laser lines, particularly P(24)e, may have better specificity, but are likely to remain wholly inadequate for the ICOGS method to be competitive with other existing technologies.

ACKNOWLEDGMENTS

The authors thank The National Energy Technology Laboratory at the U.S. Dept. of Energy (Award DE-FE0001535) and the Columbia University Research Initiative for Science and Engineering for their generous support and Philipp Stoelting for technical consultation. Roseline Polle and Arthur Reboul also thank the Alliance Program for their sponsorship.

SUPPLEMENTAL ONLINE MATERIAL

Circuit diagrams and printed circuit board layouts are included as supporting information http://dx.doi.org/10.1017/RDC.2016.5

REFERENCES

Bachor HA, Manson PJ, Sandeman RJ. 1982. Optogalvanic detection as a quantitative method in spectroscopy. *Optics Communications* 43(5): 337–42.

Berglund M, Thornell G, Persson A. 2013. Microplasma source for optogalvanic spectroscopy of nanogram samples. *Journal of Applied Physics* 114(3):033302.

Berglund M, Persson A, Thornell G. 2014. Operation characteristics and optical emission distribution of a miniaturized silicon through-substrate split-ring resonator microplasma source. *Journal of Microelectromechanical Systems* 23(6):1340–5.

Bradley L, Soohoo K, Freed C. 1986. Absolute frequencies of lasing transitions in nine CO_2 isotopic species. *IEEE Journal of Quantum Electronics* 22:234–67.

Eilers G, Persson A, Gustavsson C, Ryderfors L, Mukhtar E, Possnert G, Salehpour M. 2013. The radiocarbon intracavity optogalvanic spectroscopy setup at Uppsala. *Radiocarbon* 55(3–4):237–50.

Freed C, Bradley LC, O'Donnell R. 1980. Absolute frequencies of lasing transitions in seven CO_2 isotopic species. *IEEE Journal of Quantum Electronics* 16(11):1195–206.

Galli I, Bartalini S, Borri S, Cancio P, Mazzotti D, De Natale P, Giusfredi G. 2011a. Molecular gas sensing below parts per trillion: radiocarbon-dioxide optical detection. *Physical Review Letters* 107(27):270802.

Galli I, Pastor PC, Di Lonardo G, Fusina L, Giusfredi G, Mazzotti D, Tamassia F, De Natale P. 2011b. The v_3 band of $^{14}C^{16}O_2$ molecule measured by optical-frequency-comb-assisted cavity ring-down spectroscopy. *Molecular Physics* 109(17–18):2267–72.

Galli I, Bartalini S, Cancio P, De Natale P, Mazzotti D, Giusfredi G, Fedi M, Mando P. 2013. Optical detection of radiocarbon dioxide: first results and AMS intercomparison. *Radiocarbon* 55(2–3):213–3.

Hellborg R, Skog G. 2008. Accelerator mass spectrometry. *Mass Spectrometry Reviews* 27(5):398–427.

Ilkmen E, Murnick DE. 2010. High sensitivity laboratory based ^{14}C analysis for drug discovery. *Journal of Labelled Compounds & Radiopharmaceuticals* 53(5–6):304–7.

Litherland AE, Zhao XL, Kieser WE. 2011. Mass spectrometry with accelerators. *Mass Spectrometry Reviews* 30(6):1037–72.

Mazzotti D, Bartalini S, Borri S, Cancio P, Galli I, Giusfredi G, De Natale P. 2012. All-optical radiocarbon dating. *Optics and Photonics News* 23(12):52.

Murnick DE, Okil JO. 2005. Use of the optogalvanic effect (OGE) for isotope ratio spectrometry of $^{13}CO_2$ and $^{14}CO_2$. *Isotopes in Environmental and Health Studies* 41(4):363–71.

Murnick DE, Dogru O, Ilkmen E. 2007. Laser based ^{14}C counting, an alternative to AMS in biological studies. *Nuclear Instruments and Methods in Physics Research B* 259(1):786–9.

Murnick DE, Dogru O, Ilkmen E. 2008. Intracavity optogalvanic spectroscopy. An analytical technique for ^{14}C analysis with subattomole sensitivity. *Analytical Chemistry* 80(13):4820–4.

Murnick D, Dogru O, Ilkmen E. 2010. ^{14}C analysis via intracavity optogalvanic spectroscopy. *Nuclear Instruments and Methods in Physics Research B* 268(7–8):708–11.

Paul D, Meijer HAJ. 2015. Intracavity optogalvanic spectroscopy is not suitable for ambient level

radiocarbon detection. *Analytical Chemistry* 87(17):9025–32.

Persson A, Salehpour M. 2015. Intracavity optogalvanic spectroscopy: Is there any evidence of a radiocarbon signal? *Nuclear Instruments and Methods in Physics Research B* 361:8–12.

Persson A, Eilers G, Ryderfors L, Mukhtar E, Possnert G, Salehpour M. 2013. Evaluation of intracavity optogalvanic spectroscopy for radiocarbon measurements. *Analytical Chemistry* 85(14):6790–8.

Persson A, Berglund M, Salehpour M. 2014a. Improved optogalvanic detection with voltage biased Langmuir probes. *Journal of Applied Physics* 116(24):243301.

Persson A, Berglund M, Thornell G, Possnert G, Salehpour M. 2014b. Stripline split-ring resonator with integrated optogalvanic sample cell. *Laser Physics Letters* 11(4):045701.

Picqué N, Gueye F, Guelachvili G, Sorokin E, Sorokina IT. 2005. Time-resolved Fourier transform intracavity spectroscopy with a Cr^{2+}:ZnSe laser. *Optics Letters* 30(24):3410–2.

Povinec PP, Litherland AE, von Reden KF. 2009. Developments in radiocarbon technologies: from the Libby counter to compound-specific AMS analyses. *Radiocarbon* 51(1):45–78.

Rothman L, Gordon I, Babikov Y, Barbe A, Benner DC, Bernath P, Birk M, Bizzocchi L, Boudon V, Brown L. 2013. The HITRAN2012 molecular spectroscopic database. *Journal of Quantitative Spectroscopy and Radiative Transfer* 130:4–50.

Shrivastava A, Gupta VB 2011. Methods for the determination of limit of detection and limit of quantitation of the analytical methods. *Chronicles of Young Scientists* 2(1):21.

https://doi.org/10.1017/RDC.2016.5 Published online by Cambridge University Press